

DOI:10.12025/j.issn.1008-6358.2018.20170826

· 短篇论著 ·

两种弥散图像采集方式对胰腺神经内分泌肿瘤和实性假乳头状瘤的鉴别诊断

郭英龙, 陈财忠, 张晶晶, 孙伟, 宋旭豪, 姚秀忠*

复旦大学附属中山医院放射科, 上海市影像医学研究所, 上海 200032

[摘要] 目的: 评价憋气和呼吸门控弥散图像采集方式对胰腺实性假乳头状瘤和神经内分泌肿瘤的鉴别诊断价值。

方法: 纳入 15 例实性假乳头状瘤及 17 例神经内分泌肿瘤, 均经手术病理证实。应用 3.0T 磁共振扫描仪, 对患者进行基于自旋回波-平面回波成像的 DWI 序列扫描, 在上下、前后及左右三轴上给予 b 值为 600 s/mm^2 弥散梯度。患者均采用憋气和呼吸门控弥散图像采集方式。其中, 呼吸门控模式在弥散梯度前加 220 ms 恢复时间、 180° 角的翻转梯度脉冲。比较两组弥散图像伪影情况及病变组织的表观弥散系数(ADC)值, 分析两种弥散图像对胰腺实性假乳头状瘤和神经内分泌肿瘤的鉴别价值。

结果: 呼吸门控模式下伪影评分低于憋气模式, 差异有统计学意义($P=0.000$)。憋气模式下, 胰腺神经内分泌肿瘤的 ADC 值高于实性假乳头状瘤, 但差异无统计学意义; 呼吸门控模式下, 神经内分泌肿瘤的 ADC 值高于实性假乳头状瘤, 差异有统计学意义($P=0.000$)。结论: 与憋气方式相比较, 呼吸门控弥散图像采集方式对胰腺神经内分泌肿瘤和实性假乳头状瘤肿瘤的鉴别诊断价值更优。

[关键词] 胰腺; 磁共振; 弥散图像; 呼吸门控

[中图分类号] R 735.9

[文献标志码] A

Two diffusion weighted imaging modes for differential diagnosis of pancreatic neuroendocrine tumor and solid-pseudopapillary tumor

GUO Ying-long, CHEN Cai-zhong, ZHANG Jing-jing, SUN Wei, SONG Xu-hao, YAO Xiu-zhong*

Department of Radiology, Zhongshan Hospital, Fudan University, Shanghai Institute of Medical Imaging, Shanghai 200032, China

[Abstract] Objective: To investigate the differential value of two diffusion weighted imaging using respiratory-gating and breath-hold methods for differential diagnosis of pancreatic neuroendocrine tumor (PNET) and solid-pseudopapillary tumor (SPT). Methods: Fifteen cases of SPT and 17 cases of PNET were enrolled in this study, and all were proven by histopathology. A 3.0T magnetic resonance scanner was used. On the basis of spin echo-echo planar imaging sequence, a diffusion gradient with a b value of 600 s/mm^2 was applied in three axes. Diffusion weighted imaging methods included respiratory gating and breath-holding. A gradient pulse with an angle of 180° and 220 ms inversion recovery time was conducted before turning to diffusion gradient pulse for the respiratory-gated signal acquisitions. Pancreatic artifacts and ADC value of the lesions were compared between the two methods, and the differential diagnosis value of the two methods for SPT and PNET were evaluated. Results: Pancreatic artifacts were less observed using the respiratory-gating mode compared with the breath-holding mode, with a statistical difference ($P=0.000$). For the breath-holding mode, the ADC value of PNET was higher than that of SPT, but no statistical difference was observed. For respiratory-gating mode, the ADC value of PNET was statistically higher than that of SPT ($P=0.000$). Conclusions: Diffusion weighted imaging with the respiratory-gating mode is superior to the breath-holding mode for the differential diagnosis of SPT and PNET.

[Key Words] pancreas; magnetic resonance; diffusion weighted imaging; respiratory-gating

磁共振扩散加权成像通过对组织中水分子的布朗运动进行量化评估, 从而对组织病理特征进行

评价。该成像技术常被用于肿瘤的诊断、鉴别及疗效随访^[1-6]。在腹部器官应用磁共振技术时, 弥散图

[收稿日期] 2017-09-22

[接受日期] 2018-04-13

[基金项目] 上海市自然科学基金(16ZR1405900). Supported by Natural Science Foundation of Shanghai (16ZR1405900).

[作者简介] 郭英龙, 技师. E-mail: 573356648@qq.com

*通信作者(Corresponding author). Tel: 021-64041990; E-mail: fjqzyaoxz02@163.com

像的采集常采用憋气模式。但是,该种方式下,患者呼吸运动、肠蠕动及血管搏动等因素可能造成影像失真。

此外,应用常规影像常难以在术前准确鉴别胰腺肿瘤,如胰腺神经内分泌肿瘤(pancreatic neuroendocrine tumor, PNET)与实性假乳头状瘤(solid-pseudopapillary tumor of the pancreas, SPT)^[7-9]。表观弥散系数(apparent diffusion coefficient, ADC)稳定性和鉴别诊断的有效性对于弥散加权成像的稳定和保真有重要意义。弥散图像的采集除应用较多的憋气模式外,还有呼吸门控模式^[10-11]。本研究应用3.0T磁共振扫描仪,比较两种弥散图像采集方式在PNET和SPT中的应用价值,以寻求更好地保证磁共振扩散加权成像质量的图像采集模式,提高鉴别诊断的价值。

1 资料与方法

1.1 一般资料 2012年1月至2016年12月在我院经手术病例证实的17例PNET患者和15例SPT患者。PNET患者中,男性7例,女性10例;年龄17~68岁,平均46.3岁。SPT患者中,男性4例,女性11例;年龄15~41岁,平均24.7岁。

1.2 检查方法 采用3.0T磁共振扫描仪(Signa HDX, GE Medical Systems, Milwaukee, Wis, USA),胰腺扫描时使用8个通道的相控阵腹部表面线圈。所有研究对象在磁共振检查前禁水和食物6 h;进行呼吸训练,使呼吸幅度和频率保持稳定。检查过程中,呼吸信号位置曲线高位时,通过憋气模式采集图像;憋气模式下弥散图像自动生成后,在呼吸门控模式下进行弥散成像,呼吸信号位置曲线高位时采集。

三平面定位后,行常规T₁加权成像、T₂加权成像、弥散加权成像及三维T₁加权成像平扫和增强扫描。弥散序列均基于自旋回波-平面回波成像序列。呼吸门控模式:重复时间7 500 ms,回波时间60 ms,三轴位弥散梯度脉冲,加速因子2,采集次数6,层厚5 mm,层间距2 mm,带宽250 kHz,FOV 400 mm×280 mm,矩阵130×96;在弥散图像采集前给予翻转时间为220 ms的180°翻转脉冲,扫描时间192 s。憋气采集模式:重复时间2 300 ms,回波时间52 ms,三轴位弥散梯度脉冲,加速因子2,采集次数2,层厚5 mm,层间距2 mm,带宽250 kHz,FOV 400 mm×280 mm,130×96矩阵,扫描时间

18 s。

1.3 数据分析 评价2种弥散图像采集序列每个层面的伪影程度,包括胰腺和病变层面,对每一层面进行伪影记分。每一层面伪影评分之和除以分析层面数所得的值为该病例的伪影评分,该分析过程由2位高年资磁共振医师进行。伪影评分标准:0分为图像质量好,无伪影;1分为图像质量较好,可以进行ADC值的测量;2分为图像质量差,无法进行ADC值测量,胰腺轮廓及病灶完整;3分为图像质量差,无法进行ADC值测量,胰腺或病灶缺如、断层及轮廓扭曲。

所有数据测量和分析均在GE Advantage Workstation 4.3工作站进行。参照T₁加权图像、T₂加权图像及增强T₁加权图像,选取足够大的兴趣区(region of interest, ROI),尽量避开非肿瘤组织实质性区(正常胰腺、病灶边缘)、肿瘤囊变坏死区以及伪影。测量并记录2种采集模式采集的弥散图像中肿瘤的ADC值。

1.4 统计学处理 采用SPSS 18.0软件进行统计。ADC值以 $\bar{x}\pm s$ 表示,两组间比较采用t检验(方差齐时)或 χ^2 检验(方差不齐时),检验水准(α)为0.05。

2 结果

2.1 两种采集模式下图像伪影的比较 呼吸门控模式下图像伪影少(图1A),能检出胰腺肿瘤,评分为(0.47±0.23)分;憋气模式下伪影较多,可掩盖肿瘤(图1B),评分为(1.13±0.39)分。2种模式下伪影评分差异有统计学意义($P=0.000$,表1)。

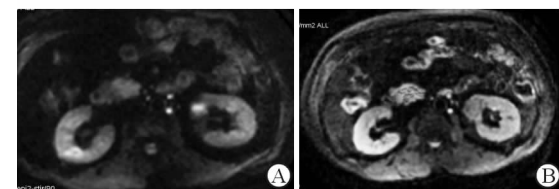


图1 胰头神经内分泌肿瘤的弥散加权成像

A: 呼吸门控模式下,显示胰头肿瘤;B: 憋气模式,胰头伪影掩盖肿瘤

2.2 两种图像采集模式下PNET和SPT肿瘤ADC值的比较 憋气模式下,PNET的ADC值高于SPT,但差异无统计学意义(χ^2 值=17.329, $P=0.083$)。呼吸门控模式下,PNET的ADC值高于SPT,差异有统计学意义($t=20.673$, $P=0.000$,表1)。

表1 两种采集模式下弥散图像的伪影评分和肿瘤ADC值比较

采集模式	伪影评分/分	ADC/(10 ³ mm ² ·s ⁻¹)	
		SPT(n=15)	PNET(n=17)
憋气	1.13±0.39	1.27±0.31	1.84±0.67
呼吸门控	0.47±0.23*	1.04±0.39	1.71±0.37△

ADC: 表观弥散系数; SPT: 胰腺实性假乳头状瘤; PNET: 胰腺神经内分泌肿瘤。*P=0.000与憋气模式相比; △P=0.000与同模式下SPT组相比

3 讨 论

随着3.0T磁共振日益普及,其磁场强梯度增加,信噪比(SNR)随之增加,但磁敏感伪影也增加,且更易受到呼吸等活动的影响,使其在腹部肿瘤中的应用更加困难。研究^[12-13]采用憋气弥散图像采集模式进行胰腺扩散加权成像,发现随着b值的增加,胰腺的覆盖范围缩小、层面厚度、层间隔增加,从而导致漏诊;憋气模式还可导致胰腺显像伪影增加、胰腺及病变的信号强度不等,使诊断价值降低。本研究中,相对于憋气模式,呼吸门控模式下的正常胰腺区域为低信号、肿瘤为高信号,两者对比明显,且伪影少、ADC值差异有统计学意义,说明呼吸模式有助于胰腺肿瘤的筛查与鉴别诊断。

呼吸门控采集模式下成像时间比憋气模式下长,因此可以在弥散图像采集前,执行1个恢复时间为220 ms及翻转角为180°的脉冲。经过翻转脉冲和220 ms恢复时间后,再进行对称性弥散梯度脉冲,激发组织的水分子布朗运动,此时胰腺、肿瘤组织及胃肠系膜脂肪的高信号伪影减少,对ADC值的影响减少。而憋气采集模式扫描时间短,不能应用翻转脉冲,周围组织的信号不能被抑制,使胰腺内信号不均匀,ADC值增加。

SPT是多发生于年轻女性患者的少见低度恶性肿瘤,少数发生于老年女性及男性患者。发生于年轻女性的SPT有典型的影像学表现,容易诊断。发生于年轻女性的SPT为有包膜、易出血、体积较大的囊实质性肿瘤,动态增强后实质性区呈渐进性延迟强化特征;当PNET发生出血、囊变及钙化时,易与SPT混淆。发生于男性及老年女性的SPT多表现为非囊性、分界清楚、无包膜的小均质肿块,很难与PNET鉴别。

由于PNET血供丰富,血流灌注效应较强,其憋气模式下的图像ADC值可高于SPT。但是,憋气模式下采集的图像伪影多,ADC值可能失真,进而导致两者的ADC值差异无统计学意义。呼吸门

控采集模式的弥散图像伪影少、ADC值相对准确,能反映水分子运动在肿瘤内的受限程度。SPT与PNET间质含量均较少,细胞密集程度相似,但是后者血流灌注效应明显大于前者^[14-15]。本研究中,呼吸门控模式下,PNET的ADC值高于SPT(P=0.000)。

综上所述,呼吸门控采集模式下的弥散图像伪影少,其显像效果优于憋气模式,有助于PNET和SPT的鉴别。

参考文献

- BADER A, HERAN M, DUNHAM C, et al. Radiological features of infantile glioblastoma and desmoplastic infantile tumors: British Columbia's Children's Hospital experience [J]. J Neurosurg Pediatr, 2015, 16(2):119-125.
- BARENTSZ M W, TAVIANI V, CHANG J M, et al. Assessment of tumor morphology on diffusion-weighted (DWI) breast MRI: diagnostic value of reduced field of view DWI[J]. J Magn Reson Imaging, 2015, 42(6):1656-1665.
- XU Q G, XIAN J F. Role of quantitative magnetic resonance imaging parameters in the evaluation of treatment response in malignant tumors[J]. Chin Med J (Engl), 2015, 128(8):1128-1133.
- MIRKA H, KORCAKOVA E, KASTNER J, et al. Diffusion-weighted imaging using 3.0 T MRI as a possible biomarker of renaltumors[J]. Anticancer Res, 2015, 35(4):2351-2357.
- SVOLOS P, KOUSI E, KAPSALAKI E, et al. The role of diffusion and perfusion weighted imaging in the differential diagnosis of cerebral tumors: a review and future perspectives[J]. Cancer Imaging, 2014, 14:20.
- SCHELHORN J, BEST J, REINBOLDT M P, et al. Does diffusion-weighted imaging improve therapy response evaluation in patients with hepatocellular carcinoma after radioembolization? Comparison of MRI using Gd-EOB-DTPA with and without DWI[J]. J Magn Reson Imaging, 2015, 42(3):818-827.
- FUKUKURA Y, SHINDO T, HAKAMADA H, et al. Diffusion-weighted MR imaging of the pancreas: optimizing b-value for visualization of pancreatic adenocarcinoma[J]. Eur Radiol, 2016, 26(10):3419-3427.
- OHARA Y, ODA T, HASHIMOTO S, et al. Pancreatic neuroendocrine tumor and solid-pseudopapillary neoplasm: Key immunohistochemical profiles for differential diagnosis [J]. World J Gastroenterol, 2016, 22(38):8596-8604.
- IMPERIALE A, ADDEO P, AVEROUS G, et al. Solid pseudopapillary pancreatic tumor mimicking a neuroendocrine neoplasm on ¹⁸F-FDOPA PET/CT[J]. J Clin Endocrinol Metab, 2013, 98(7):2643-2644.

- [10] MERIDEN Z, SHI C, EDIL B H, et al. Hyaline globules in neuroendocrine and solid-pseudopapillary neoplasms of the pancreas: a clue to the diagnosis [J]. Am J Surg Pathol, 2011, 35(7):981-988.
- [11] SAREMI F, JALILI M, SEFIDBAKHT S, et al. Diffusion-weighted imaging of the abdomen at 3 T: image quality comparison with 1.5-T magnet using 3 different imaging sequences [J]. J Comput Assist Tomogr, 2011, 35(3):317-325.
- [12] MURAOKA N, UEMATSU H, KIMURA H, et al. Apparent diffusion coefficient in pancreatic cancer characterization and histopathological correlations [J]. J Magn Reson Imaging, 2008, 27(6):1302-1308.
- [13] FATTAH R, BALCI N C, PERMAN W H, et al. Pancreatic diffusion-weighted imaging (DWI): comparison between mass-forming focal pancreatitis (FP), pancreatic cancer (PC), and normal pancreas [J]. J Magn Reson Imaging, 2009, 29(2):350-356.
- [14] MOMTAHEN AJ, BALCI NC, ALKAADE S, et al. Focal pancreatitis mimicking pancreatic mass: magnetic resonance imaging (MRI)/magnetic resonance cholangiopancreatography (MRCP) findings including diffusion-weighted MRI [J]. Acta Radiol, 2008, 49(5):490-497.
- [15] LEE S S, BYUN J H, PARK B J, et al. Quantitative analysis of diffusion-weighted magnetic resonance imaging of the pancreas: usefulness in characterizing solid pancreatic masses [J]. J Magn Reson Imaging, 2008, 28(4):928-936.

〔本文编辑〕姬静芳

DOI:10.12025/j.issn.1008-6358.2018.20180294

· 短篇论著 ·

育龄妇女皮下埋植避孕的临床疗效分析

季丹

上海市长宁区妇幼保健院产科, 上海 200090

〔摘要〕 目的:探讨皮下埋植避孕的临床疗效及其对育龄妇女的不良反应,为提高皮下埋植避孕效用提供数据支持。**方法:**纳入2015年1月至2016年6月接受皮下埋植避孕的育龄妇女200例,每隔90 d进行1次电话随访,记录其避孕效果和不良反应。**结果:**187例有效样本中,皮下埋植避孕成功率95.2%。随访期间45例发生不良反应,不良反应发生率为24.1%。出血异常为最常见的不良反应(64.4%),其次为类早孕反应(13.3%)。出血异常的29例受试者中,出血次数减少发生最多(11例)。**结论:**皮下埋植避孕临床避孕效果好,在合理控制其不良反应的情况下,适合推广使用。

〔关键词〕 育龄妇女;皮下埋植避孕;不良反应;出血模式

〔中图分类号〕 R 169.41 **〔文献标志码〕** A

Analysis of clinical effect and adverse reactions of subcutaneous implantation contraception for women of childbearing age

JI Dan

Department of Obstetrics, Chang Ning District Maternal and Child Health Care Hospital, Shanghai 200090, China

〔Abstract〕 Objective: To investigate the clinical effect and adverse reactions of subcutaneous implantation contraception for women of childbearing age, and provide evidence support for contraceptive efficacy of subcutaneous implantation. **Methods:** A total of 200 women of childbearing age who accepted subcutaneous implantation contraception in our hospital between January 2015 and June 2016 were included in the study. A telephone follow-up was conducted every 90 days to record the contraceptive effect and adverse reactions. **Results:** The success rate of subcutaneous implantation contraception was 95.2%. Forty-five adverse reactions were recorded during the follow-up period, with a incidence of 24.1%. The most common adverse reaction was abnormal bleeding (64.4%), followed by early pregnancy reaction (13.3%). Bleeding reduction was the most common type of abnormal bleeding (11/29). **Conclusions:** The clinical contraceptive effect of subcutaneous implantation is acceptable, and it is suitable for popularization and use under the condition of reasonable control of its adverse reactions.

〔收稿日期〕 2018-03-27

〔接受日期〕 2018-06-10

〔作者简介〕 季丹,主治医师. E-mail: drjidan331@sina.com